Kinematics, dynamics and control design of 4WIS4WID mobile robots

Ming-Han Lee, Tzuu-Hseng S. Li

aiRobots Laboratory, Department of Electrical Engineering, National Cheng Kung University, 1 University Road, Tainan, Taiwan 70101
E-mail: thsli@mail.ncku.edu.tw

Published in *The Journal of Engineering*; Received on 2nd September 2014; Accepted on 30th October 2014

Abstract: Kinematic and dynamic modelling and corresponding control design of a four-wheel-independent steering and four-wheel-independent driving (4WIS4WID) mobile robot are presented in this study. Different from the differential or car-like mobile robot, the 4WIS4WID mobile robot is controlled by four steering and four driving motors, so the control scheme should possess the ability to integrate and manipulate the four independent wheels. A trajectory tracking control scheme is developed for the 4WIS4WID mobile robot, where both non-linear kinematic control and dynamic sliding-mode control are designed. All of the stabilities of the kinematic and dynamic control laws are proved by Lyapunov stability analysis. Finally, the feasibility and validity of the proposed trajectory tracking control scheme are confirmed through computer simulations.

1 Introduction

Many structures of vehicles or mobile robots have been presented, such as two-wheel-steering (2WS), four-wheel-steering (4WS), differential wheel, skid-steer and omni-directional drive. In recent years, because of the rapid expansion of electric motors and their high manoeuvrability, vehicles or mobile robots based on the four-wheel-independent steering and four-wheel-independent driving (4WIS4WID) structure have been presented and researched in many areas such as transportation, agriculture and service industry.

The 2WS or car-like structure [1–4] is like that of a traditional car, but in this structure only the front wheels can steer and they are coupled by mechanical linkages. The 4WS [5, 6] can steer the front wheels and rear wheels, but the wheels are coupled with mechanical linkages so that whether they are 2WS or 4WS, the steering angles are limited and are restricted by their mechanical structures. This limitation means that the vehicles or robots of 2WS or 4WS cannot implement some motions, for example, lateral moving.

The differential wheeled mobile robot [7–11] has two parallel driving wheels on the right side and left side of the robot and one or two caster wheels to balance the robot. The two driving wheels drive independently, and this type of robot uses the velocity difference between the two wheels to turn the direction and move. Another similar type is skid-steer, which uses the same way of driving, but different from the differential wheeled mobile robot, it may have four or more driving wheels [12, 13] or be equipped with tracks [14] without castor wheels such as skid-steer loaders or backhoes.

The omni-directional mobile robots [15–18] are equipped with omni wheels so that they can move in any direction instantly without turning the direction of the wheels or changing the robot orientation. Although this type has high manoeuvrability, it still has some disadvantages. The first disadvantage is that all the wheels do not roll in the direction of the robot movement, so the efficiency is low. The second disadvantage is omni-wheel itself contains many wheels/rollers which lead greater resistance to rotate and imply greater loss of energy.

There are some vehicles and wheeled mobile robots, Nissan Pivo 2, Nissan Pivo 3, Toyota Fine-T, Toyota Fine-X, humanoid robot Justin [19], OK-1 [20], Care-O-bot 3 [21] and others [22–24] which adopt the 4WIS4WID structure. The 4WIS4WID mobile robot is equipped with four wheels, but the four wheels are not coupled by mechanical linkages. Each wheel is steered independently using a motor, which is equipped between the body and each wheel of the mobile robot. On the basis of the structure of the 4WIS4WID mobile robot, the manoeuvrability is more diversified so it can implement some motions such as lateral moving or zero-turn radius. The 4WIS4WID mobile robot can achieve the same actions as car-like, 4WS and skid-steer mobile robots. Moreover, the 4WIS4WID mobile robot can also implement the same motions as the omni-directional mobile robot. However, the 4WIS4WID mobile robot has to turn the orientation of wheels so it cannot instantly move in any direction like the omni-directional mobile robot.

The first purpose of this paper is to present the kinematic and dynamic models, which can be utilised to design controllers to deal with control issues for 4WIS4WID mobile robot. The 4WIS4WID mobile robot has high manoeuvrability; the control problem is more complex because it has to manipulate four-wheel motors and four steering motors to move smoothly. Reference [25] presents an omni-directional steer-by-wire system to control the steering angle of four wheels, where the instantaneous centre of rotation (ICR) is considered. When robot moves straight, the ICR is undefined or infinite. This disadvantage means that the control law has to be distinguished into three conditions, turning right, moving straight and turning left; then it has to switch them. The kinematic control method proposed in [26] is also based on the ICR, where one extra control mode has to be induced when the desired rotational velocity of mobile robot is zero. Furthermore, the velocity control scheme developed in [26] also needs to be divided into three control modes based on three conditions. In [27], Selekwa and Nistler proposed a kinematic control law to control the steering angle and wheel velocity of four wheels, where the virtual rear and front steering angles should be given first. This phenomenon limits its application. Moreover, if the virtual rear or front steering angle is zero, the wheel steering angle cannot be calculated. If the steering angle of any wheel is zero, the wheel velocity cannot be calculated or is infinite.

To design a better controller for the 4WIS4WID mobile robot, we present a kinematic model that includes eleven state variables, and a dynamic model, which is developed by the Lagrangian equation. On the basis of the proposed models, we design a controller that combines kinematic control with dynamic control to implement the trajectory tracking control problem. Through the non-linear kinematic control law, the velocity and steering angle of every wheel can be determined appropriately. In dynamic control law, this paper proposes a trajectory tracking control scheme based on sliding-mode control (SMC) to reduce the tracking error with system uncertainties and external disturbances. The SMC and its extensions have been applied to many kinds of mobile robots [5, 28–30].

This is an open access article published by the IET under the Creative Commons Attribution License (http://creativecommons.org/licenses/by/3.0/)

doi: 10.1049/joe.2014.0241

The main contributions of this paper are as follows: (i) both kinematic and dynamic models of the 4WIS4WID mobile robot are developed. They can help researchers to design and develop other controllers and/or applications for the 4WIS4WID mobile robot. (ii) both non-linear kinematic control and SMC-based dynamic control schemes for the trajectory tracking problem of 4WIS4WID mobile robot are presented and the stabilities are confirmed by the Lyapunov stability theory. Moreover, the comparison with the proportional–integral (PI) dynamic control is given. (iii) both the model and control system are not examined based on the concept of ICR, so the control algorithm is not necessarily divided into some conditions addressed in the literature [25, 26].

The organisation of this paper is as follows: in Section 2, both the kinematic and dynamic models of the 4WIS4WID mobile robot are addressed. Section 3 describes the trajectory tracking problem for the 4WIS4WID mobile robot. Furthermore, the kinematic and dynamic controllers are presented. The trajectory tracking simulation results based on the proposed control scheme proposed are illustrated in Section 4. Finally, Section 5 gives conclusions.

2 System description

This section presents the kinematic and dynamic models of the 4WIS4WID mobile robot. One can find that the concept of ICR is not necessary to setup these models.

2.1 Kinematic model

A simplified 4WIS4WID mobile robot system with four wheels, without considering the motions of pitch, roll and heave, is shown in Fig. 1 and the configuration is depicted in Fig. 2. The robot is driven by four-wheel motors and through another four motors to turn these four-wheel motors. x, y and θ are the postures of the robot in the world coordinate frame; w_i denotes the wheel i; δ_i denotes the steering angle of wheel i; a and b are, respectively, the length between the centroid of the robot and each wheel. Before developing the model of 4WIS4WID mobile robot, three configurations for the robot are assumed as below.

Assumption 1: The position of the four wheels in the robot coordinate frame is predefined as $(x_{w1}^r, y_{w1}^r) = (a, b)$, $(x_{w2}^r, y_{w2}^r) = (-a, b)$, $(x_{w3}^r, y_{w3}^r) = (-a, -b)$ and $(x_{w4}^r, y_{w4}^r) = (a, -b)$. The (x_{wi}^r, y_{wi}^r) denotes the coordinates of wheel i in the robot coordinate frame. v and v_i are, respectively, the linearity velocity of the robot and wheel i, where $v = \sqrt{v_x^2 + v_y^2}$ and $v_i = \sqrt{v_{xi}^2 + v_{yi}^2}$. ω is the angular velocity of the robot's body. ω_i is the steering velocity of wheel i.

Assumption 2: The positions of centre of mass and centroid of the 4WIS4WID mobile robot are the same.

Assumption 3: Both the radius and mass of all wheels are assumed to be the same.

Under no slipping condition, the relationships of the velocity between each wheel and the body of robot are obtained by the rigid body constraint for the robot which are represented as

$$v_{xi} = v_i \cos(\delta_i) = v_x - y_{wi}^r \omega \tag{1}$$

$$v_{yi} = v_i \sin(\delta_i) = v_y + x_{wi}^r \omega \tag{2}$$

By substituting the parameters of the four wheels into (1) and (2), the relationship of the four wheels and body of the robot can be represented as

$$\boldsymbol{P}\begin{bmatrix} v_x \\ v_y \\ \omega \end{bmatrix} = \boldsymbol{X}\begin{bmatrix} v_1 \\ v_2 \\ v_3 \\ v_4 \end{bmatrix} \tag{3}$$

where $\boldsymbol{P} = \begin{bmatrix} 1 & 0 & -b \\ 0 & 1 & a \\ 1 & 0 & -b \\ 0 & 1 & -a \\ 1 & 0 & b \\ 0 & 1 & -a \\ 1 & 0 & b \\ 0 & 1 & a \end{bmatrix}$, $\boldsymbol{X} = \begin{bmatrix} c(\delta_1) & 0 & 0 & 0 \\ s(\delta_1) & 0 & 0 & 0 \\ 0 & c(\delta_2) & 0 & 0 \\ 0 & s(\delta_2) & 0 & 0 \\ 0 & 0 & c(\delta_3) & 0 \\ 0 & 0 & s(\delta_3) & 0 \\ 0 & 0 & 0 & c(\delta_4) \\ 0 & 0 & 0 & s(\delta_4) \end{bmatrix}$,

and where $c(\cdot)$ and $s(\cdot)$ denote the trigonometric functions cos(·) and sin(·), respectively. Moreover, the pseudo-inverse matrix of $\boldsymbol{P}$ is as follows

$$\boldsymbol{P}^+ = \begin{bmatrix} 1/4 & 0 & 1/4 & 0 & 1/4 & 0 & 1/4 & 0 \\ 0 & 1/4 & 0 & 1/4 & 0 & 1/4 & 0 & 1/4 \\ -\frac{b}{K} & \frac{a}{K} & -\frac{b}{K} & -\frac{a}{K} & \frac{b}{K} & -\frac{a}{K} & \frac{b}{K} & \frac{a}{K} \end{bmatrix}$$

where $K = 4a^2 + 4b^2$. Premultiply (3) by $\boldsymbol{P}^+$, one can obtain the relationship of the four wheels and robot's body as follows

$$\begin{bmatrix} v_x \\ v_y \\ \omega \end{bmatrix} = \begin{bmatrix} \frac{c(\delta_1)}{4} & \frac{c(\delta_2)}{4} & \frac{c(\delta_3)}{4} & \frac{c(\delta_4)}{4} \\ \frac{s(\delta_1)}{4} & \frac{s(\delta_2)}{4} & \frac{s(\delta_3)}{4} & \frac{s(\delta_4)}{4} \\ \frac{1}{W_1} & \frac{1}{W_2} & \frac{1}{W_3} & \frac{1}{W_4} \end{bmatrix}\begin{bmatrix} v_1 \\ v_2 \\ v_3 \\ v_4 \end{bmatrix} \tag{4}$$

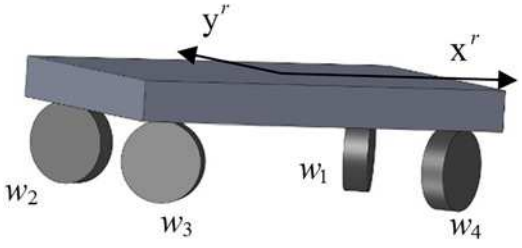


Fig. 1 *4WIS4WID robot system*

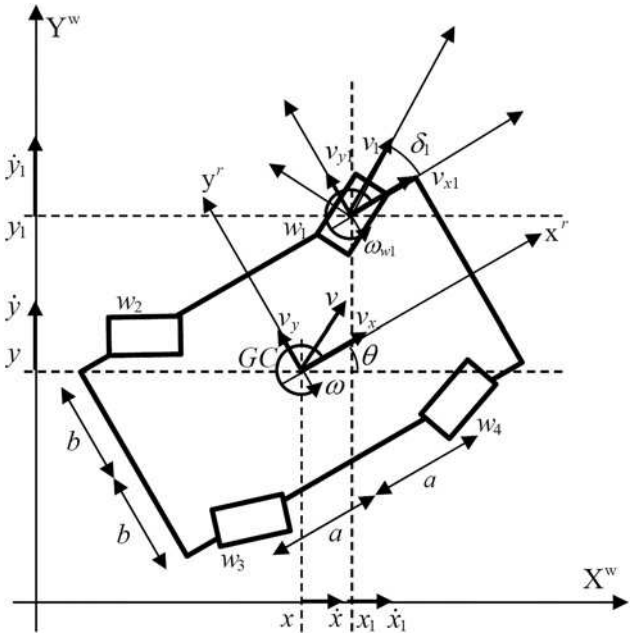


Fig. 2 *Configuration of 4WIS4WID robot system in world coordinate frame*

This is an open access article published by the IET under the Creative Commons Attribution License (http://creativecommons.org/licenses/by/3.0/)

20513305, 2015, 1, Downloaded from https://ietresearch.onlinelibrary.wiley.com/doi/10.1049/joe.2014.0241, Wiley Online Library on [26/08/2026]. See the Terms and Conditions (https://onlinelibrary.wiley.com/terms-and-conditions) on Wiley Online Library for rules of use; OA articles are governed by the applicable Creative Commons License

where $W_i = \left(-y_{wi}^r c(\delta_i) + x_{wi}^r s(\delta_i)\right)/\left(4(x_{wi}^r)^2 + 4(y_{wi}^r)^2\right)$. Note that $\boldsymbol{P}^+\boldsymbol{P} = \boldsymbol{I}_3$, where $\boldsymbol{I}_3 \in \Re^{3\times 3}$ is the identity matrix.

Combining the three states of the robot body, wheel rotating angle and wheel steering angle, there are 11 state variables to represent the position and posture of the mobile robot

$$\boldsymbol{q} = \begin{bmatrix} x & y & \theta & \varphi_1 & \varphi_2 & \varphi_3 & \varphi_4 & \delta_1 & \delta_2 & \delta_3 & \delta_4 \end{bmatrix}^{\mathrm{T}} \quad (5)$$

After some calculations, one can obtain the kinematic model of 4WIS4WID mobile robot as follows

$$\begin{aligned} \dot{\boldsymbol{q}} &= \begin{bmatrix} \dot{x} \\ \dot{y} \\ \dot{\theta} \\ \dot{\varphi}_1 \\ \dot{\varphi}_2 \\ \dot{\varphi}_3 \\ \dot{\varphi}_4 \\ \dot{\delta}_1 \\ \dot{\delta}_2 \\ \dot{\delta}_3 \\ \dot{\delta}_4 \end{bmatrix} = \begin{bmatrix} \frac{c_1}{4} & \frac{c_2}{4} & \frac{c_3}{4} & \frac{c_4}{4} & 0 & 0 & 0 & 0 \\ \frac{s_1}{4} & \frac{s_2}{4} & \frac{s_3}{4} & \frac{s_4}{4} & 0 & 0 & 0 & 0 \\ W_1 & W_2 & W_3 & W_4 & 0 & 0 & 0 & 0 \\ r^{-1} & 0 & 0 & 0 & 0 & 0 & 0 & 0 \\ 0 & r^{-1} & 0 & 0 & 0 & 0 & 0 & 0 \\ 0 & 0 & r^{-1} & 0 & 0 & 0 & 0 & 0 \\ 0 & 0 & 0 & r^{-1} & 0 & 0 & 0 & 0 \\ 0 & 0 & 0 & 0 & 1 & 0 & 0 & 0 \\ 0 & 0 & 0 & 0 & 0 & 1 & 0 & 0 \\ 0 & 0 & 0 & 0 & 0 & 0 & 1 & 0 \\ 0 & 0 & 0 & 0 & 0 & 0 & 0 & 1 \end{bmatrix} \begin{bmatrix} v_1 \\ v_2 \\ v_3 \\ v_4 \\ \omega_1 \\ \omega_2 \\ \omega_3 \\ \omega_4 \end{bmatrix} \\ &= \boldsymbol{J}\boldsymbol{v} \end{aligned} \quad (6)$$

where $\dot{\boldsymbol{q}}$ is defined as the velocity vector in the world coordinate frame; φ_i denotes the angular of wheel i; c_i and s_i are represented as $\cos(\delta_i + \theta)$ and $\sin(\delta_i + \theta)$, respectively.

2.2 Dynamic model

To derive the dynamic model, the kinetic energy of the mobile robot is described as

$$\begin{aligned} E &= E_x + E_y + E_\theta + E_\varphi + E_\delta \\ &= \frac{1}{2}m_{\mathrm{b}}v_x^2 + \frac{1}{2}m_{\mathrm{b}}v_x^2 + \frac{1}{2}I_\theta\dot{\theta}^2 \\ &\quad + \frac{1}{2}\sum_{i=1}^{4}\left(m_{\mathrm{w}}v_i^2 + I_\varphi\dot{\varphi}_i^2\right) + \frac{1}{2}\sum_{i=1}^{4}I_\delta\dot{\delta}^2 \\ &= \frac{1}{2}m_{\mathrm{b}}v_x^2 + \frac{1}{2}m_{\mathrm{b}}v_x^2 + \frac{1}{2}I_\theta\dot{\theta}^2 \\ &\quad + \frac{1}{2}\sum_{i=1}^{4}\left(m_{\mathrm{w}}\left(v_{ix}^2 + v_{iy}^2\right) + I_\varphi\dot{\varphi}_i^2\right) + \frac{1}{2}\sum_{i=1}^{4}I_\delta\dot{\delta}^2 \\ &= \frac{1}{2}m_{\mathrm{b}}v_x^2 + \frac{1}{2}m_{\mathrm{b}}v_x^2 + \frac{1}{2}I_\theta\dot{\theta}^2 \\ &\quad + \frac{m_{\mathrm{w}}}{2}\sum_{i=1}^{4}\left(4v_x^2 + 4v_y^2 + 4\left(a_i^2 + b_i^2\right)\dot{\theta}^2\right) \\ &\quad + \frac{I_\varphi}{2}\sum_{i=1}^{4}\dot{\varphi}_i^2 + \frac{I_\delta}{2}\sum_{i=1}^{4}\dot{\delta}^2 \\ &= \frac{1}{2}mv_x^2 + \frac{1}{2}mv_y^2 + \frac{1}{2}I\dot{\theta}^2 + \frac{I_\varphi}{2}\sum_{i=1}^{4}\dot{\varphi}_i^2 + \frac{I_\delta}{2}\sum_{i=1}^{4}\dot{\delta}^2 \end{aligned} \quad (7)$$

where m_{b} and m_{w} are, respectively, the weight of the robot's body and each wheel; I_θ, I_φ and I_δ are the moment of inertia about the rotating of the robot's body, the rolling of the wheel and the steering of the wheel, respectively; $m = m_{\mathrm{b}} + 4m_{\mathrm{w}}$ and $I = I_\theta + 4m_{\mathrm{w}}(a^2 + b^2)$.

Owing to $v_x^2 + v_y^2 = \dot{x}^2 + \dot{y}^2$, (7) can be rewritten as

$$E = \frac{1}{2}m\dot{x}^2 + \frac{1}{2}m\dot{y}^2 + \frac{1}{2}I\dot{\theta}^2 + \frac{I_\varphi}{2}\sum_{i=1}^{4}\dot{\varphi}_i^2 + \frac{I_\delta}{2}\sum_{i=1}^{4}\dot{\delta}^2 \quad (8)$$

Without considering the disturbances, the Lagrange formula is used to derive the dynamic equation

$$\frac{\mathrm{d}}{\mathrm{d}t}\left(\frac{\partial E}{\partial \dot{\boldsymbol{q}}_j}\right) - \frac{\partial E}{\partial \boldsymbol{q}_j} + \boldsymbol{F}(\dot{\boldsymbol{q}}) + \boldsymbol{\tau}_{\mathrm{d}} = \boldsymbol{N}(q)\boldsymbol{\tau}, \quad (j = 1,\ 2,\ 3,\ \ldots,\ 11) \quad (9)$$

where τ is the torque input vector, $\boldsymbol{F}(\dot{\boldsymbol{q}})$ denotes the surface friction forces and $\boldsymbol{\tau}_{\mathrm{d}}$ is the bounded disturbances. After doing some calculations, the dynamic model is obtained and represented as follows

$$\boldsymbol{M}\dot{\boldsymbol{q}} + \boldsymbol{V}_{\boldsymbol{m}}\dot{\boldsymbol{q}} + \boldsymbol{F} + \boldsymbol{\tau}_{\mathrm{d}} = \boldsymbol{N}\boldsymbol{\tau} \quad (10)$$

The metrics in (10) are represented as

$$\boldsymbol{M} = \mathrm{diag}\{m,\ m,\ I,\ I_\varphi,\ I_\varphi,\ I_\varphi,\ I_\varphi,\ I_\delta,\ I_\delta,\ I_\delta,\ I_\delta\}$$

$$\boldsymbol{V}_m = 0$$

$$\boldsymbol{N} = \begin{bmatrix} \frac{c_1}{r} & \frac{c_2}{r} & \frac{c_3}{r} & \frac{c_4}{r} & 0 & 0 & 0 & 0 \\ \frac{s_1}{r} & \frac{s_2}{r} & \frac{s_3}{r} & \frac{s_4}{r} & 0 & 0 & 0 & 0 \\ T_1 & T_2 & T_3 & T_4 & 0 & 0 & 0 & 0 \\ 1 & 0 & 0 & 0 & 0 & 0 & 0 & 0 \\ 0 & 1 & 0 & 0 & 0 & 0 & 0 & 0 \\ 0 & 0 & 1 & 0 & 0 & 0 & 0 & 0 \\ 0 & 0 & 0 & 1 & 0 & 0 & 0 & 0 \\ 0 & 0 & 0 & 0 & 1 & 0 & 0 & 0 \\ 0 & 0 & 0 & 0 & 0 & 1 & 0 & 0 \\ 0 & 0 & 0 & 0 & 0 & 0 & 1 & 0 \\ 0 & 0 & 0 & 0 & 0 & 0 & 0 & 1 \end{bmatrix}$$

$$\boldsymbol{F} = \begin{bmatrix} f_{\mathrm{d}\varphi_1} & f_{\mathrm{d}\varphi_2} & f_{\mathrm{d}\varphi_3} & f_{\mathrm{d}\varphi_4} & f_{\mathrm{d}\delta_1} & f_{\mathrm{d}\delta_2} & f_{\mathrm{d}\delta_3} & f_{\mathrm{d}\delta_4} \end{bmatrix}^{\mathrm{T}}$$

$$\boldsymbol{\tau}_{\mathrm{d}} = \begin{bmatrix} \tau_{\mathrm{d}\varphi_1} & \tau_{\mathrm{d}\varphi_2} & \tau_{\mathrm{d}\varphi_3} & \tau_{\mathrm{d}\varphi_4} & \tau_{\mathrm{d}\delta_1} & \tau_{\mathrm{d}\delta_2} & \tau_{\mathrm{d}\delta_3} & \tau_{\mathrm{d}\delta_4} \end{bmatrix}^{\mathrm{T}}$$

and

$$\boldsymbol{\tau} = \begin{bmatrix} \tau_{\varphi_1} & \tau_{\varphi_2} & \tau_{\varphi_3} & \tau_{\varphi_4} & \tau_{\delta_1} & \tau_{\delta_2} & \tau_{\delta_3} & \tau_{\delta_4} \end{bmatrix}^{\mathrm{T}}$$

where diag is the abbreviation of diagonal matrix; $T_i = r^{-1}[x_i s(\delta_i) - y_i c(\delta_i)]$; $f_{\mathrm{d}\varphi_i}$ and $f_{\mathrm{d}\delta_i}$ are the friction forces affected on the rolling and steering wheel i, respectively; $\tau_{\mathrm{d}\varphi_i}$ and $\tau_{\mathrm{d}\delta_i}$ are the bounded disturbances affected on the rolling and steering wheel i, respectively; and τ_{φ_i} and τ_{δ_i} are the torques to roll and steer wheel i, respectively. Differentiating (6) and substituting into (10), then multiplying the result by $\boldsymbol{J}^{\mathrm{T}}$, (10) is transferred into another form as follows

$$\bar{\boldsymbol{M}}(\boldsymbol{q})\dot{\boldsymbol{v}} + \bar{\boldsymbol{V}}_{\boldsymbol{m}}(\boldsymbol{q})\boldsymbol{v} + \bar{\boldsymbol{F}} + \bar{\boldsymbol{\tau}}_{\mathrm{d}} = \bar{\boldsymbol{N}}(\boldsymbol{q})\boldsymbol{\tau} \quad (11)$$

where $\bar{\boldsymbol{M}} = \boldsymbol{J}^{\mathrm{T}}\boldsymbol{M}\boldsymbol{J} \in \Re^{8\times 8}$, $\bar{\boldsymbol{V}}_m = \boldsymbol{J}^{\mathrm{T}}\boldsymbol{M}\dot{\boldsymbol{J}} \in \Re^{8\times 8}$, $\bar{\boldsymbol{F}} = \boldsymbol{J}^{\mathrm{T}}\boldsymbol{F} \in \Re^{8\times 1}$, $\bar{\boldsymbol{\tau}}_{\mathrm{d}} = \boldsymbol{J}^{\mathrm{T}}\boldsymbol{\tau}_{\mathrm{d}} \in \Re^{8\times 1}$ and $\bar{\boldsymbol{N}} = \boldsymbol{J}^{\mathrm{T}}\boldsymbol{N} \in \Re^{8\times 8}$.

This is an open access article published by the IET under the Creative Commons Attribution License (http://creativecommons.org/licenses/by/3.0/)

20513305, 2015, 1, Downloaded from https://ietresearch.onlinelibrary.wiley.com/doi/10.1049/joe.2014.0241, Wiley Online Library on [26/08/2026]. See the Terms and Conditions (https://onlinelibrary.wiley.com/terms-and-conditions) on Wiley Online Library for rules of use; OA articles are governed by the applicable Creative Commons License

The variables of $\bar{\boldsymbol{M}}$, $\bar{\boldsymbol{V}}_m$ and $\bar{\boldsymbol{N}}$ are

$$\bar{\boldsymbol{M}} = \begin{bmatrix} \bar{M}_{11} & \bar{M}_{21} & \bar{M}_{31} & \bar{M}_{41} & 0 & 0 & 0 & 0 \\ \bar{M}_{21} & \bar{M}_{22} & \bar{M}_{32} & \bar{M}_{42} & 0 & 0 & 0 & 0 \\ \bar{M}_{31} & \bar{M}_{32} & \bar{M}_{33} & \bar{M}_{43} & 0 & 0 & 0 & 0 \\ \bar{M}_{41} & \bar{M}_{42} & \bar{M}_{43} & \bar{M}_{44} & 0 & 0 & 0 & 0 \\ 0 & 0 & 0 & 0 & I_\delta & 0 & 0 & 0 \\ 0 & 0 & 0 & 0 & 0 & I_\delta & 0 & 0 \\ 0 & 0 & 0 & 0 & 0 & 0 & I_\delta & 0 \\ 0 & 0 & 0 & 0 & 0 & 0 & 0 & I_\delta \end{bmatrix}$$

$$\bar{M}_{ii} = IW_i^2 + \frac{m}{16}\left(c_i^2 + s_i^2\right) + \frac{I_\varphi}{r^2}, \quad i = 1,\ 2,\ 3,\ 4$$

$$\bar{M}_{ij} = IW_jW_i + \frac{m}{16}\left(c_jc_i + s_js_i\right)$$

$$i = 2,\ 3,\ 4;\ j = 1,\ 2,\ 3,\ 4;\ i \neq j$$

$$\bar{\boldsymbol{V}}_m = \begin{bmatrix} \bar{V}_{11} & \bar{V}_{21} & \bar{V}_{31} & \bar{V}_{41} & 0 & 0 & 0 & 0 \\ \bar{V}_{21} & \bar{V}_{22} & \bar{V}_{32} & \bar{V}_{42} & 0 & 0 & 0 & 0 \\ \bar{V}_{31} & \bar{V}_{23} & \bar{V}_{33} & \bar{V}_{43} & 0 & 0 & 0 & 0 \\ \bar{V}_{32} & \bar{V}_{24} & \bar{V}_{34} & \bar{V}_{44} & 0 & 0 & 0 & 0 \\ 0 & 0 & 0 & 0 & 0 & 0 & 0 & 0 \\ 0 & 0 & 0 & 0 & 0 & 0 & 0 & 0 \\ 0 & 0 & 0 & 0 & 0 & 0 & 0 & 0 \\ 0 & 0 & 0 & 0 & 0 & 0 & 0 & 0 \end{bmatrix}$$

$$\bar{V}_{ij} = IW_j\dot{W}_i + m\left(c_j\dot{c}_i + s_j\dot{s}_i\right)/16$$

$$i = 1,\ 2,\ 3,\ 4;\ j = 1,\ 2,\ 3,\ 4$$

$$\bar{\boldsymbol{N}} = \begin{bmatrix} \bar{N}_{11} & \bar{N}_{21} & \bar{N}_{31} & \bar{N}_{41} & 0 & 0 & 0 & 0 \\ \bar{N}_{21} & \bar{N}_{22} & \bar{N}_{32} & \bar{N}_{42} & 0 & 0 & 0 & 0 \\ \bar{N}_{31} & \bar{N}_{23} & \bar{N}_{33} & \bar{N}_{43} & 0 & 0 & 0 & 0 \\ \bar{N}_{32} & \bar{N}_{24} & \bar{N}_{34} & \bar{N}_{44} & 0 & 0 & 0 & 0 \\ 0 & 0 & 0 & 0 & 1 & 0 & 0 & 0 \\ 0 & 0 & 0 & 0 & 0 & 1 & 0 & 0 \\ 0 & 0 & 0 & 0 & 0 & 0 & 1 & 0 \\ 0 & 0 & 0 & 0 & 0 & 0 & 0 & 1 \end{bmatrix}$$

$$\bar{N}_{ii} = \frac{W_i(y_ic(\delta_i) + x_is(\delta_i))}{r} + \frac{s_i^2 + c_i^2}{4r} + \frac{1}{r}, \quad i = 1,\ 2,\ 3,\ 4$$

and

$$\bar{N}_{ij} = \frac{W_i(y_jc(\delta_j) + x_js(\delta_j))}{r} + \frac{s_is_j + c_ic_j}{4r}$$
$$i = 1,\ 2,\ 3,\ 4;\ j = 1,\ 2,\ 3,\ 4;\ i \neq j$$

Property 1: $\bar{\boldsymbol{M}}$ is a symmetric positive-definite matrix.

Property 2: $\dot{\bar{\boldsymbol{M}}} - 2\bar{\boldsymbol{V}}_m$ is the skew symmetric.

Premultiply (11) by $\bar{\boldsymbol{M}}^{-1}$ and regarding the friction forces $\bar{\boldsymbol{F}}$ and disturbances torques $\bar{\boldsymbol{\tau}}_\mathrm{d}$ as the system uncertainties and disturbances, then the dynamic equation of the 4WIS4WID can be described as

$$\begin{aligned} \dot{\boldsymbol{v}}(t) &= -\bar{\boldsymbol{M}}^{-1}\bar{\boldsymbol{V}}_m\boldsymbol{v}(t) + \bar{\boldsymbol{M}}^{-1}\bar{\boldsymbol{N}}\boldsymbol{\tau}(t) - \bar{\boldsymbol{M}}^{-1}\bar{\boldsymbol{F}} - \bar{\boldsymbol{M}}^{-1}\bar{\boldsymbol{\tau}}_\mathrm{d} \\ &\equiv -\boldsymbol{A}\boldsymbol{v}(t) + \boldsymbol{B}\boldsymbol{\tau}(t) + \boldsymbol{d}(t) \end{aligned} \tag{12}$$

where $\boldsymbol{A} = \bar{\boldsymbol{M}}^{-1}\bar{\boldsymbol{V}}_m$, $\boldsymbol{B} = \bar{\boldsymbol{M}}^{-1}\bar{\boldsymbol{N}}$ and $\boldsymbol{d} = -\bar{\boldsymbol{M}}^{-1}\bar{\boldsymbol{F}} - \bar{\boldsymbol{M}}^{-1}\bar{\boldsymbol{\tau}}_\mathrm{d}$.

3 Trajectory tracking control design

In this section, a trajectory tracking problem of the 4WIS4WID mobile robot is discussed and both non-linear kinematic and dynamic SMC controllers for the 4WIS4WID mobile robot are designed.

3.1 Problem statement

Suppose that a reference robot $\boldsymbol{q}_\mathrm{d} = [x_\mathrm{d}(t) \quad y_\mathrm{d}(t) \quad \theta_\mathrm{d}(t)]^\mathrm{T}$ moves along a time-varying trajectory. The control objective is to let the robot track $\dot{\boldsymbol{q}}_\mathrm{d}$ and the tracking error between the reference robot and the actual robot approach zero. On the basis of this objective, the main task is to design a control law for the 4WIS4WID mobile robot to ensure the actual robot is able to track the reference one.

3.2 Kinematic controller design

Before designing the controllers, the vector of the tracking error is defined as follows

$$\begin{aligned} \boldsymbol{q}_\mathrm{e} &= \begin{bmatrix} x_\mathrm{e} \\ y_\mathrm{e} \\ \theta_\mathrm{e} \end{bmatrix} = \boldsymbol{R}(\theta)\cdot\tilde{\boldsymbol{q}}_\mathrm{e} \\ &= \begin{bmatrix} \cos\theta & \sin\theta & 0 \\ -\sin\theta & \cos\theta & 0 \\ 0 & 0 & 1 \end{bmatrix}\begin{bmatrix} x_\mathrm{d} - x \\ y_\mathrm{d} - y \\ \theta_\mathrm{d} - \theta \end{bmatrix} \end{aligned} \tag{13}$$

and the tracking error dynamic is denoted as

$$\dot{\boldsymbol{q}}_\mathrm{e} = \dot{\boldsymbol{q}}_\mathrm{d} - \dot{\boldsymbol{q}} = \begin{bmatrix} \dot{x}_\mathrm{e} & \dot{y}_\mathrm{e} & \dot{\theta}_\mathrm{e} \end{bmatrix}^\mathrm{T} \tag{14}$$

where $\boldsymbol{R}(\theta)$ is the rotation matrix. After some computing, $\dot{\boldsymbol{q}}_\mathrm{e}$ can be derived as follows

$$\begin{aligned} C\dot{\boldsymbol{q}}_\mathrm{e} &= \begin{bmatrix} y_\mathrm{e}\dot{\theta} + v_{x\mathrm{d}} - v_x \\ -x_\mathrm{e}\dot{\theta} + v_{y\mathrm{d}} - v_y \\ \omega_\mathrm{d} - \omega \end{bmatrix} \\ &= \begin{bmatrix} y_\mathrm{e}\dot{\theta} + \frac{1}{4}\sum_{i=1}^{4}(v_{i\mathrm{d}}\cos\delta_{i\mathrm{d}}) - \frac{1}{4}\sum_{i=1}^{4}(v_i\cos\delta_i) \\ -x_\mathrm{e}\dot{\theta} + \frac{1}{4}\sum_{i=1}^{4}(v_{i\mathrm{d}}\sin\delta_{i\mathrm{d}}) - \frac{1}{4}\sum_{i=1}^{4}(v_i\sin\delta_i) \\ \sum_{i=1}^{4}(v_{i\mathrm{d}}W_{i\mathrm{d}}) - \sum_{i=1}^{4}(v_iW_i) \end{bmatrix} \end{aligned} \tag{15}$$

where $v_{i\mathrm{d}} = \sqrt{v_{x\mathrm{id}}^2 + v_{y\mathrm{id}}^2}$, $\delta_{i\mathrm{d}} = \arctan2(v_{y\mathrm{id}}, v_{x\mathrm{id}})$, $W_{i\mathrm{d}} = \left(-y_{wi}^rc(\delta_{i\mathrm{d}}) + x_{wi}^rs(\delta_{i\mathrm{d}})\right) / \left(4\left(x_{wi}^r\right)^2 + 4\left(y_{wi}^r\right)^2\right)$, $v_{x\mathrm{id}} = v_{x\mathrm{d}} - y_{wi}^r\omega_\mathrm{d}$ and $v_{y\mathrm{id}} = v_{y\mathrm{d}} + x_{wi}^r\omega_\mathrm{d}$.

The kinematic tracking control law for the 4WIS4WID mobile robot is derived as follows. Define the Lyapunov function candidate as

$$V_k = \frac{1}{2}\left(x_\mathrm{e}^2 + y_\mathrm{e}^2 + \theta_\mathrm{e}^2\right) \geq 0 \tag{16}$$

This is an open access article published by the IET under the Creative Commons Attribution License (http://creativecommons.org/licenses/by/3.0/)

20513305, 2015, 1, Downloaded from https://ietresearch.onlinelibrary.wiley.com/doi/10.1049/joe.2014.0241, Wiley Online Library on [26/08/2026]. See the Terms and Conditions (https://onlinelibrary.wiley.com/terms-and-conditions) on Wiley Online Library for rules of use; OA articles are governed by the applicable Creative Commons License

Taking the time derivative of V_k implies

$$\begin{aligned}\dot{V}_k &= x_e\dot{x}_e + y_e\dot{y}_e + \theta_e\dot{\theta}_e \\ &= x_e\left[\frac{1}{4}\sum_{i=1}^{4}(v_{id}\cos\delta_{id}) - \frac{1}{4}\sum_{i=1}^{4}(v_i\cos\delta_i)\right] \\ &\quad + y_e\left[\frac{1}{4}\sum_{i=1}^{4}(v_{id}\sin\delta_{id}) - \frac{1}{4}\sum_{i=1}^{4}(v_i\sin\delta_i)\right] \\ &\quad + \theta_e\left[\sum_{i=1}^{4}(v_{id}W_{id}) - \sum_{i=1}^{4}(v_iW_i)\right]\end{aligned} \tag{17}$$

Let the control laws be defined as

$$v_{ic} = z_1\sqrt{a_i^2 + b_i^2} \tag{18}$$

$$\delta_{ic} = z_2 + \arctan 2(b_i,\ a_i) \tag{19}$$

where $a_i = v_{id}\cos\delta_{id} + k_x x_e - k_\theta y_{wi}\theta_e$ and $b_i = v_{id}\sin\delta_{id} + k_y y_e + k_\theta x_{wi}\theta_e$; k_x, k_y and k_θ are all positive constants; both z_1 and z_2 are defined as

$$(z_1,\ z_2) = \begin{cases}(+1,\ 0), & |\delta_{id} - \delta_i| \le \pi/2 \\ (-1,\ \pi), & \text{otherwise}\end{cases} \tag{20}$$

By substituting both (18) and (19) into (17), one can obtain the results as follows.

Although $(z_1, z_2) = (+1, 0)$, then

$$\begin{aligned}&\sum_{i=1}^{4}(v_{id}\cos\delta_{id} - v_i\cos\delta_i) \\ &\quad = \sum_{i=1}^{4}\left(v_{id}\cos\delta_{id} - \sqrt{a_i^2 + b_i^2}\,\frac{a_i}{\sqrt{a_i^2 + b_i^2}}\right) \\ &\quad = \sum_{i=1}^{4}(-k_x x_e + k_\theta y_{wi}\theta_e) = -4k_x x_e\end{aligned} \tag{21}$$

$$\begin{aligned}&\sum_{i=1}^{4}(v_{id}\sin\delta_{id} - v_i\sin\delta_i) \\ &\quad = \sum_{i=1}^{4}\left(v_{id}\sin\delta_{id} - \sqrt{a_i^2 + b_i^2}\cdot\frac{b_i}{\sqrt{a_i^2 + b_i^2}}\right) \\ &\quad = \sum_{i=1}^{4}(-k_y y_e - k_\theta x_{wi}\theta_e) = -4k_y y_e\end{aligned} \tag{22}$$

$$\begin{aligned}&\sum_{i=1}^{4}(v_{id}W_{id}) - \sum_{i=1}^{4}(v_iW_i) \\ &\quad = \frac{1}{4}\sum_{i=1}^{4}\left(-\frac{y^r_{wi}\left(-k_x x_e + k_\theta y^r_{wi}\theta_e\right)}{(x^r_{wi})^2 + (y^r_{wi})^2} + \frac{x^r_{wi}\left(-k_y y_e - k_\theta x^r_{wi}\theta_e\right)}{(x^r_{wi})^2 + (y^r_{wi})^2}\right) \\ &\quad = \frac{1}{4}\sum_{i=1}^{4}\left(-\frac{k_\theta\theta_e(y^r_{wi})^2 + k_\theta\theta_e(x^r_{wi})^2}{(x^r_{wi})^2 + (y^r_{wi})^2}\right) \\ &\quad = -k_\theta\theta_e\end{aligned} \tag{23}$$

Although $(z_1, z_2) = (-1, \pi)$, then

$$\begin{aligned}&\sum_{i=1}^{4}(v_{id}\cos\delta_{id} - v_i\cos\delta_i) \\ &\quad = \sum_{i=1}^{4}\left[v_{id}\cos\delta_{id} - \left(-\sqrt{a_i^2 + b_i^2}\cdot -\frac{a_i}{\sqrt{a_i^2 + b_i^2}}\right)\right] \\ &\quad = \sum_{i=1}^{4}(-k_x x_e + k_\theta y_{wi}\theta_e) = -4k_x x_e\end{aligned} \tag{24}$$

$$\begin{aligned}&\sum_{i=1}^{4}(v_{id}\sin\delta_{id} - v_i\sin\delta_i) \\ &\quad = \sum_{i=1}^{4}\left[v_{id}\sin\delta_{id} - \left(-\sqrt{a_i^2 + b_i^2}\cdot -\frac{b_i}{\sqrt{a_i^2 + b_i^2}}\right)\right] \\ &\quad = \sum_{i=1}^{4}(-k_y y_d - k_\theta x_{wi}\theta_e) = -4k_y y_e\end{aligned} \tag{25}$$

and

$$\begin{aligned}&\sum_{i=1}^{4}(v_{id}W_{id}) - \sum_{i=1}^{4}(v_iW_i) \\ &\quad = \frac{1}{4}\sum_{i=1}^{4}\left(-\frac{y^r_{wi}\left(-k_x x_e + k_\theta y^r_{wi}\theta_e\right)}{(x^r_{wi})^2 + (y^r_{wi})^2} + \frac{x^r_{wi}\left(-k_y y_e - k_\theta x^r_{wi}\theta_e\right)}{(x^r_{wi})^2 + (y^r_{wi})^2}\right) \\ &\quad = -k_\theta\theta_e\end{aligned} \tag{26}$$

According to the above results, one can find (17) becomes

$$\dot{V}_k = -4k_x x_e^2 - 4k_y y_e^2 - k_\theta\theta_e^2 \tag{27}$$

Note that (19) is the control signal of steering angle. To control the steering angle, the control input of the steering angular velocity of wheel i for the 4WIS4WID mobile robot is defined as

$$\dot{\delta}_i = \dot{\delta}_{ic} + k_{\delta_i}\delta_{ie} \tag{28}$$

where k_{δ_i} is a positive constant of wheel i.

Define the Lyapunov function candidate for the four steering angles of 4WIS4WID mobile robot as

$$V_\delta = \frac{1}{2}\sum_{i=1}^{4}\delta_{ie}^2 \ge 0 \tag{29}$$

where $\delta_{ie} = \delta_{ic} - \delta_i$. Taking the time derivative of V_δ and considering (28) imply

$$\dot{V}_\delta = \sum_{i=1}^{4}\delta_{ie}\dot{\delta}_{ie} = \sum_{i=1}^{4}\delta_{ie}\left(\dot{\delta}_{ic} - \dot{\delta}_i\right) \tag{30}$$

By choosing appropriate gains of k_x, k_y, k_θ and k_{δ_i}, $\dot{V}_k$ and $\dot{V}_\delta$ can be guaranteed less than zero for all $t \ge 0$ while $\boldsymbol{q}_e \ne 0$ and $\delta_{ie} \ne 0$. Therefore, using the kinematic control laws, (18), (19) and (28) to control the 4WIS4WID mobile robot, the tracking error (13) is asymptomatically stable.

This is an open access article published by the IET under the Creative Commons Attribution License (http://creativecommons.org/licenses/by/3.0/)

doi: 10.1049/joe.2014.0241

20513305, 2015, 1, Downloaded from https://ietresearch.onlinelibrary.wiley.com/doi/10.1049/joe.2014.0241, Wiley Online Library on [26/08/2026]. See the Terms and Conditions (https://onlinelibrary.wiley.com/terms-and-conditions) on Wiley Online Library for rules of use; OA articles are governed by the applicable Creative Commons License

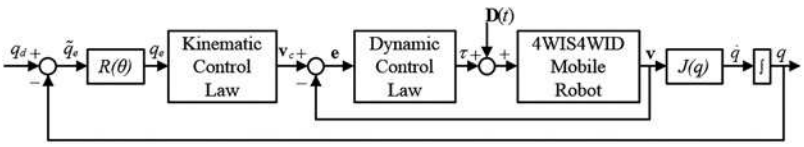


Fig. 3 *Trajectory tracking control scheme of the 4WIS4WID mobile robot*

3.3 Dynamic controller design

In this section, a dynamic tracking controller, SMC, will be designed for the 4WIS4WID mobile robot. Define the velocity error as

$$\boldsymbol{e} = \begin{bmatrix} e_{\varphi_1} \\ e_{\varphi_2} \\ e_{\varphi_3} \\ e_{\varphi_4} \\ e_{\delta_1} \\ e_{\delta_2} \\ e_{\delta_3} \\ e_{\delta_4} \end{bmatrix} = \begin{bmatrix} v_{1c} \\ v_{2c} \\ v_{3c} \\ v_{4c} \\ \dot{\delta}_{1c} \\ \dot{\delta}_{2c} \\ \dot{\delta}_{3c} \\ \dot{\delta}_{4c} \end{bmatrix} - \begin{bmatrix} v_1 \\ v_2 \\ v_3 \\ v_4 \\ \dot{\delta}_1 \\ \dot{\delta}_2 \\ \dot{\delta}_3 \\ \dot{\delta}_4 \end{bmatrix} = \boldsymbol{v}_c(t) - \boldsymbol{v}(t) \tag{31}$$

and by choosing a PI-like sliding surface as

$$\begin{aligned} \boldsymbol{S}(t) &= \begin{bmatrix} s_1 & s_2 & s_3 & s_4 & s_5 & s_6 & s_7 & s_8 \end{bmatrix}^{\mathrm{T}} \\ &= \boldsymbol{e} + \boldsymbol{\lambda} \int_0^t \boldsymbol{e}(\tau)\, \mathrm{d}\tau \end{aligned} \tag{32}$$

where $\boldsymbol{\lambda} \in \Re^{8\times 8}$ is a diagonal positive-definite matrix and $\boldsymbol{\lambda}$ is selected to stabilise the sliding surface. Although the sliding surface $\boldsymbol{S}(t)$ approaches zero, the tracking errors will also converge to zero. Therefore, the objective is to design a controller to let the system errors reach on the sliding surface. To derivate the equivalent control laws $\boldsymbol{\tau}_{\mathrm{eq}}(t)$, both the uncertainties and disturbances are assumed to be zero. The time derivative of (32) is

$$\dot{\boldsymbol{S}}(t) = \dot{\boldsymbol{e}} + \boldsymbol{\lambda e} = \dot{\boldsymbol{v}}_c(t) + \boldsymbol{A}\dot{\boldsymbol{v}}(t) - \boldsymbol{B}\boldsymbol{\tau}(t) + \boldsymbol{\lambda e}(t) \tag{33}$$

Given $\dot{\boldsymbol{S}}(t) = 0$, then the equivalent control law $\boldsymbol{\tau}_{\mathrm{eq}}(t)$ can be obtained as follows

$$\boldsymbol{\tau}_{\mathrm{eq}}(t) = \boldsymbol{B}^{-1}(\dot{\boldsymbol{v}}_c(t) + \boldsymbol{A}\boldsymbol{v}(t) + \boldsymbol{\lambda e}(t)) \tag{34}$$

Once the $\boldsymbol{\tau}_{\mathrm{eq}}(t)$ has been determined, one should derive the auxiliary discontinuous control law $\boldsymbol{\tau}_{\mathrm{r}}(t)$ to overcome the uncertainties and disturbances of the mobile robot. Suppose that $\boldsymbol{A}$ and $\boldsymbol{B}$ have the bounded uncertain parameters and the bounded disturbances $\boldsymbol{d}(t)$ are existing, (12) is rewritten as

$$\dot{\boldsymbol{v}}(t) \equiv -\hat{\boldsymbol{A}}\boldsymbol{v}(t) + \hat{\boldsymbol{B}}\boldsymbol{\tau}(t) + \boldsymbol{d}(t) \tag{35}$$

where $\hat{\boldsymbol{A}} = \boldsymbol{A} + \boldsymbol{\Delta A}$ and $\hat{\boldsymbol{B}} = \boldsymbol{B} + \boldsymbol{\Delta B}$. $\boldsymbol{\Delta A} \in \Re^{8\times 8}$ and $\boldsymbol{\Delta B} \in \Re^{8\times 8}$ are the bounded system uncertainties which are generated by perturbations of system parameters. By considering the uncertainties and disturbances, (33) is rewritten as

$$\begin{aligned} \dot{\boldsymbol{S}}(t) &= \dot{\boldsymbol{v}}_c(t) + \hat{\boldsymbol{A}}\boldsymbol{v}(t) - \hat{\boldsymbol{B}}\boldsymbol{\tau}(t) + \boldsymbol{d}(t) + \boldsymbol{\lambda e}(t) \\ &= \dot{\boldsymbol{v}}_c(t) + (\boldsymbol{A} + \boldsymbol{\Delta A})\boldsymbol{v}(t) - (\boldsymbol{B} + \boldsymbol{\Delta B})\boldsymbol{\tau}(t) \\ &\quad + \boldsymbol{d}(t) + \boldsymbol{\lambda e}(t) \\ &= \dot{\boldsymbol{v}}_c(t) + \hat{\boldsymbol{A}}\boldsymbol{v}(t) - \hat{\boldsymbol{B}}\boldsymbol{\tau}(t) + \boldsymbol{\lambda e}(t) + (\boldsymbol{\Delta A}\boldsymbol{U}(t) \\ &\quad - \boldsymbol{\Delta B}\boldsymbol{\tau}(t) + \boldsymbol{d}(t)) \\ &= \dot{\boldsymbol{v}}_c(t) + \boldsymbol{A}\boldsymbol{v}(t) - \boldsymbol{B}\boldsymbol{\tau}(t) + \boldsymbol{\lambda e}(t) + \boldsymbol{D}(t) \end{aligned} \tag{36}$$

where $\boldsymbol{D}(t) = \boldsymbol{\Delta A}\boldsymbol{U}(t) - \boldsymbol{\Delta B}\boldsymbol{\tau}(t) + \boldsymbol{d}(t) \in \Re^{8\times 1}$, and the element D_i of $\boldsymbol{D}(t)$ is defined as $|D_i| \le \bar{D}_i$, where $\bar{D}_i$ is a bound positive constant of D_i.

Therefore, in order to ensure the system is stable, an auxiliary discontinuous control law is added and defined as

$$\boldsymbol{\tau}_{\mathrm{r}}(t) = \boldsymbol{B}^{-1}\boldsymbol{K}\mathbf{Sat}(\boldsymbol{S}) \tag{37}$$

where $\boldsymbol{K} \in \Re^{8\times 8}$ is the switch gain matrix concerned with upper bounds of uncertainties and $\boldsymbol{K}$ is positive-definite and diagonal

$$\mathbf{Sat}(\boldsymbol{S},\ \varepsilon) = \begin{bmatrix} \mathrm{sat}(s_1,\ \varepsilon) \\ \mathrm{sat}(s_2,\ \varepsilon) \\ \mathrm{sat}(s_3,\ \varepsilon) \\ \mathrm{sat}(s_4,\ \varepsilon) \\ \mathrm{sat}(s_5,\ \varepsilon) \\ \mathrm{sat}(s_6,\ \varepsilon) \\ \mathrm{sat}(s_7,\ \varepsilon) \\ \mathrm{sat}(s_8,\ \varepsilon) \end{bmatrix}$$

ε is a small positive constant and sat is the saturation function which is adopted to suppress the chattering behaviour. Sat is represented as

$$\mathrm{sat}(s_i,\ \varepsilon) = \begin{cases} \mathrm{sign}(s_i), & |s_i| > \varepsilon \\ s_i/\varepsilon, & |s_i| \le 0 \end{cases}$$

Table 1 Parameters used in simulations

Description	Symbol	Value	Unit
coordinate of wheel 1	$(x^r_{w1},\ y^r_{w1})$	(0.2, 0.25)	m
coordinate of wheel 2	$(x^r_{w2},\ y^r_{w2})$	(−0.2, 0.25)	m
coordinate of wheel 3	$(x^r_{w3},\ y^r_{w3})$	(−0.2, −0.25)	m
coordinate of wheel 4	$(x^r_{w4},\ y^r_{w4})$	(0.2, −0.25)	m
wheel radius	r	0.05	m
robot's body mass	m_b	26	kg
vehicle inertia moment	I_z	1.5	kgm^2
wheel mass	m_w	1	kg
wheel rolling torque limitation	τ_{φ_i}	5	Nm
wheel rolling inertia moment	I_φ	0.003	kgm^2
wheel steering torque limitation	τ_{δ_i}	1	Nm
wheel steering inertia moment	I_δ	0.005	kgm^2
limit of steering angle	δ_i	$(-\pi,\ \pi)$	rad

Table 2 Control parameters

Description	Symbol	Value
gains of (18) and (19)	$k_x,\ k_y,\ k_\theta$	4, 4, 3
gains of (28)	k_{δ_i}	5
integral gains of (32)	λ_i	5
gains of (37)	k_i	10

This is an open access article published by the IET under the Creative Commons Attribution License (http://creativecommons.org/licenses/by/3.0/)

20513305, 2015, 1, Downloaded from https://ietresearch.onlinelibrary.wiley.com/doi/10.1049/joe.2014.0241, Wiley Online Library on [26/08/2026]. See the Terms and Conditions (https://onlinelibrary.wiley.com/terms-and-conditions) on Wiley Online Library for rules of use; OA articles are governed by the applicable Creative Commons License

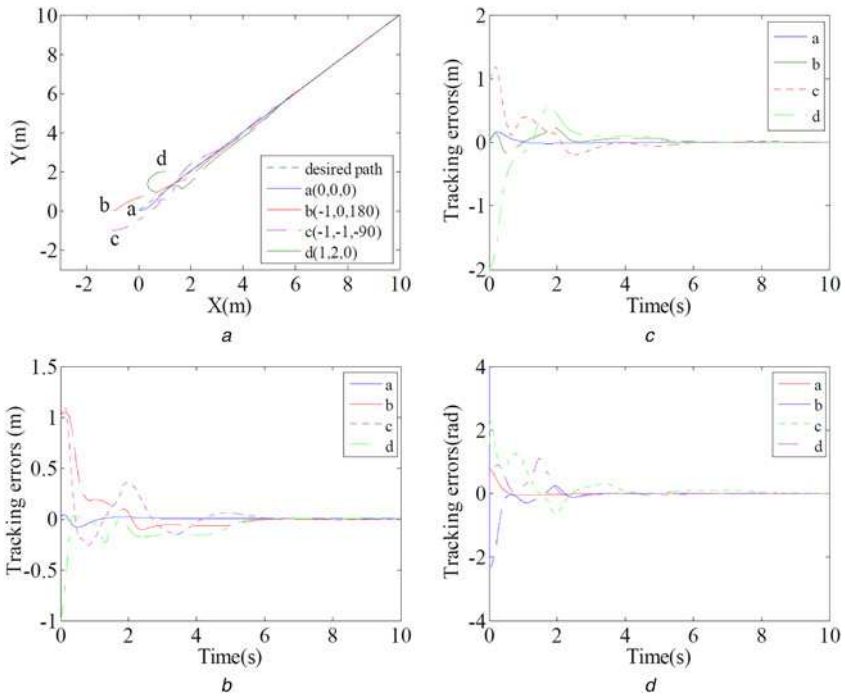


Fig. 4 *Simulation results of the straight trajectory of the four initial positions*
a x–y plot of the 4WIS4WID mobile robot
b–d Tracking errors of x_e, y_e and θ_e

The element k_{ii} in $\boldsymbol{K}$ is designed as

$$k_i = \bar{D}_i + \eta_i, \quad i = 1,\ 2,\ 3,\ \ldots,\ 8 \tag{38}$$

where $\eta_i > 0$.

Combining $\boldsymbol{\tau}_{eq}(t)$ and $\boldsymbol{\tau}_r(t)$, the consequential SMC control law for the mobile robot is

$$\begin{aligned}\boldsymbol{\tau}(t) &= \boldsymbol{\tau}_{eq}(t) + \boldsymbol{\tau}_r(t)\\ &= \boldsymbol{B}^{-1}\left(\dot{\boldsymbol{v}}_c(t) + \boldsymbol{A}\boldsymbol{v}(t) + \boldsymbol{\lambda}\boldsymbol{e}(t) + \boldsymbol{K}\cdot\mathbf{Sat}(\boldsymbol{S})\right)\end{aligned} \tag{39}$$

To show that the dynamic control law is stable for the tracking control, the Lyapunov function candidate is defined as

$$V_{SMC} = \frac{1}{2}\boldsymbol{S}^{T}(t)\boldsymbol{S}(t) \geq 0 \tag{40}$$

By taking the time derivative of V_{SMC}

$$\begin{aligned}\dot{V}_{SMC} &= \boldsymbol{S}(t)^{T}\dot{\boldsymbol{S}}(t)\\ &= \boldsymbol{S}(t)^{T}(\dot{\boldsymbol{v}}_c(t) + \boldsymbol{A}\boldsymbol{v}(t)\\ &\quad - \boldsymbol{B}\boldsymbol{\tau}(t) + \boldsymbol{\lambda}\boldsymbol{e}(t) + \boldsymbol{D}(t))\\ &= \boldsymbol{S}(t)^{T}(-\boldsymbol{K}\cdot\mathbf{Sat}(\boldsymbol{S})\\ &\quad + \boldsymbol{D}(t)) \leq \sum_{i=1}^{8}(-\eta_i|s_i(t)|)\end{aligned} \tag{41}$$

Thus, V_{SMC} is bounded for all time despite the uncertainties existed. The influence created by the uncertainties and disturbances could be reduced. According to the results of (27), (30) and (41), using the control laws (18), (19), (28) and (39), one can find that the 4WIS4WID mobile robot will converge exponentially to the reference trajectory. All of the dynamic errors satisfy $\boldsymbol{q}_e \to 0$ and $\boldsymbol{e} \to 0$ as $t \to \infty$.

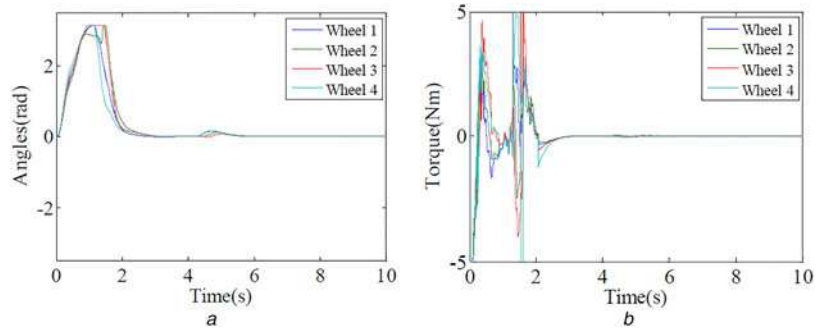


Fig. 5 *Steering angle and rolling torque of the four wheels of the initial position d*
a Steering angle
b Rolling torque

This is an open access article published by the IET under the Creative Commons Attribution License (http://creativecommons.org/licenses/by/3.0/)

20513305, 2015, 1, Downloaded from https://ietresearch.onlinelibrary.wiley.com/doi/10.1049/joe.2014.0241, Wiley Online Library on [26/08/2026]. See the Terms and Conditions (https://onlinelibrary.wiley.com/terms-and-conditions) on Wiley Online Library for rules of use; OA articles are governed by the applicable Creative Commons License

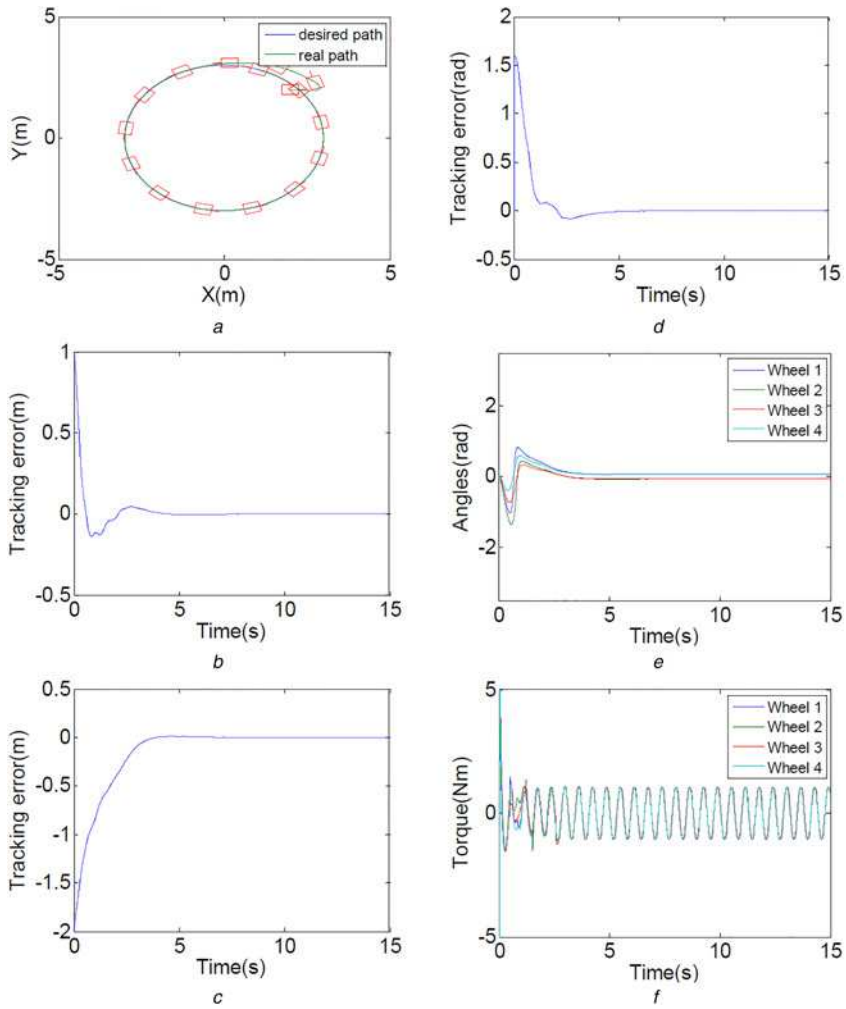


Fig. 6 *Simulation results of Case (I)*
a x–y plot of the 4WIS4WID mobile robot
b–d Tracking errors of x_e, y_e and θ_e
e Steering angle of four wheels
f Rolling torques of four wheels

The whole control scheme is shown in Fig. 3, where the inner and outer loops are used to control the dynamics and kinematics of 4WIS4WID mobile robot, respectively. The kinematic control law is implemented by equations (18), (19) and (28) and the dynamic control law is realised by (39).

4 Simulations

In this section, three computer simulations are performed to demonstrate the effectiveness and feasibility of the proposed control schemes for the 4WIS4WID mobile robot. The following simulations will define the trajectory and the initial position (X, Y, θ) of the robot. All the parameters of the mobile robot are listed in Table 1. Note that the limit of the steering angle in Table 1 means the steering motors cannot turn the wheel infinitely in the same direction because the wires used to transmit signals and power to the wheels might be twisted to breaking. They can only turn clockwise or counterclockwise in a half circle. Table 2 lists all the control parameters. In Section 4.1, a straight trajectory is used to test the feasibility of the control scheme. After the test in Section 4.2, two curvilinear trajectories are selected to demonstrate the performances using the presented control scheme.

4.1 Test by a straight trajectory

The straight trajectory utilised to test the control scheme is generated as follows

$$X_d(t) = t$$
$$Y_d(t) = t$$
$$\theta_d(t) = \arctan 2\left(\dot{Y}_d(t),\ \dot{X}_d(t)\right)$$

Four initial positions are selected to track the trajectory, which are $a(X, Y, \theta) = (0, 0, 0)$, $b(X, Y, \theta) = (-1, 0, 180°)$, $c(X, Y, \theta) = (-1, -1, -90°)$ and $d(X, Y, \theta) = (1, 2, 0)$. Fig. 4*a* shows the x–y plot of the trajectory tracking result of the four initial positions. The tracking errors of the four initial positions of the straight trajectory are shown in Figs. 4*b–d*. Figs. 5*a* and *b* represent the four-wheel steering angles and torques of the initial position $(X, Y, \theta) = (10, 3, 90°)$, respectively. One can find that as time increases, the tracking errors of this system are converging to zero. The simulation results demonstrate that the 4WIS4WID mobile robot can be stably driven using the control scheme.

This is an open access article published by the IET under the Creative Commons Attribution License (http://creativecommons.org/licenses/by/3.0/)

20513305, 2015, 1, Downloaded from https://ietresearch.onlinelibrary.wiley.com/doi/10.1049/joe.2014.0241, Wiley Online Library on [26/08/2026]. See the Terms and Conditions (https://onlinelibrary.wiley.com/terms-and-conditions) on Wiley Online Library for rules of use; OA articles are governed by the applicable Creative Commons License

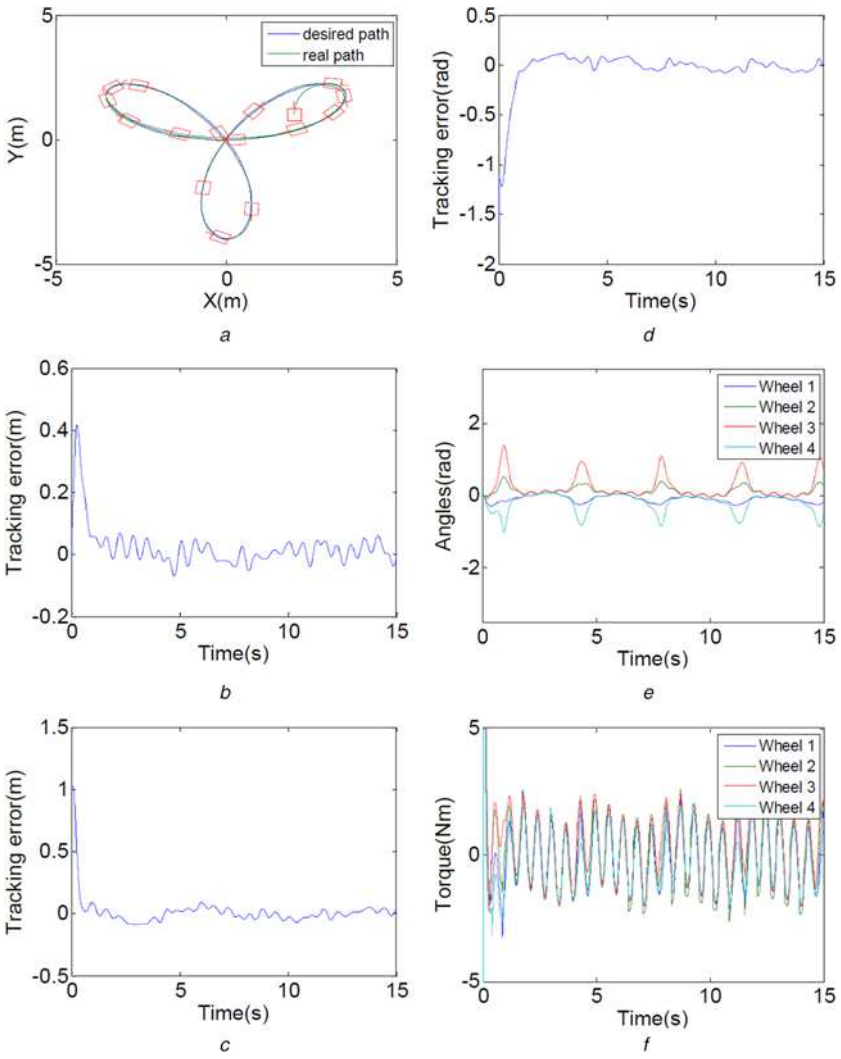


Fig. 7 *Simulation results of Case (II)*
a x–y plot of the 4WIS4WID mobile robot
b–d Tracking errors of x_e, y_e and θ_e
e Steering angle of four wheels
f Rolling torques of four wheels

4.2 Curvilinear trajectory simulations

In this section, two trajectories are utilised to demonstrate the results and performances of the proposed control schemes.

For Case (I), a circle trajectory is generated by

$$X_d(t) = 3\cos(0.5t)$$
$$Y_d(t) = 3\sin(0.5t)$$
$$\theta_d(t) = \arctan 2\left(\dot{Y}_d(t), \dot{X}_d(t)\right)$$

If the initial position of the robot is at $(X, Y, \theta) = (2, 2, 0)$ and the uncertainties and disturbances are given and bounded by

$$\boldsymbol{D}(t) = 5\sin(10t)\begin{bmatrix}1 & 1 & 1 & 1 & 1 & 1 & 1 & 1\end{bmatrix}^{\mathrm{T}}$$

Simulation results of tracking trajectory control are shown in Fig. 6, where tracking errors, four-wheel steering angles and torques are given.

For Case (II), a trajectory is generated by

$$X_d(t) = 2\sin(1.2t) + 2\cos(0.6t)$$
$$Y_d(t) = 2\sin(0.6t) + 2\cos(1.2t)$$
$$\theta_d(t) = \arctan 2\left(\dot{Y}_d(t), \dot{X}_d(t)\right)$$

The initial position of the robot is at $(X, Y, \theta) = (2, 1, 90°)$. The random uncertainties and disturbances given by the following equation are added

$$\boldsymbol{D}(t) = 5\sin(10t)\begin{bmatrix}1 & 2 & 2 & 1 & 1 & 2 & 2 & 1\end{bmatrix}^{\mathrm{T}}$$

The simulation results are shown in Fig. 7, which includes the tracking trajectory, tracking errors, four-wheel steering angles and torques.

Both simulation results demonstrate that the proposed trajectory tracking control scheme can make the 4WIS4WID mobile robot track the desired trajectories successfully and stably although the uncertainties and disturbances exist.

This is an open access article published by the IET under the Creative Commons Attribution License (http://creativecommons.org/licenses/by/3.0/)

20513305, 2015, 1, Downloaded from https://ietresearch.onlinelibrary.wiley.com/doi/10.1049/joe.2014.0241, Wiley Online Library on [26/08/2026]. See the Terms and Conditions (https://onlinelibrary.wiley.com/terms-and-conditions) on Wiley Online Library for rules of use; OA articles are governed by the applicable Creative Commons License

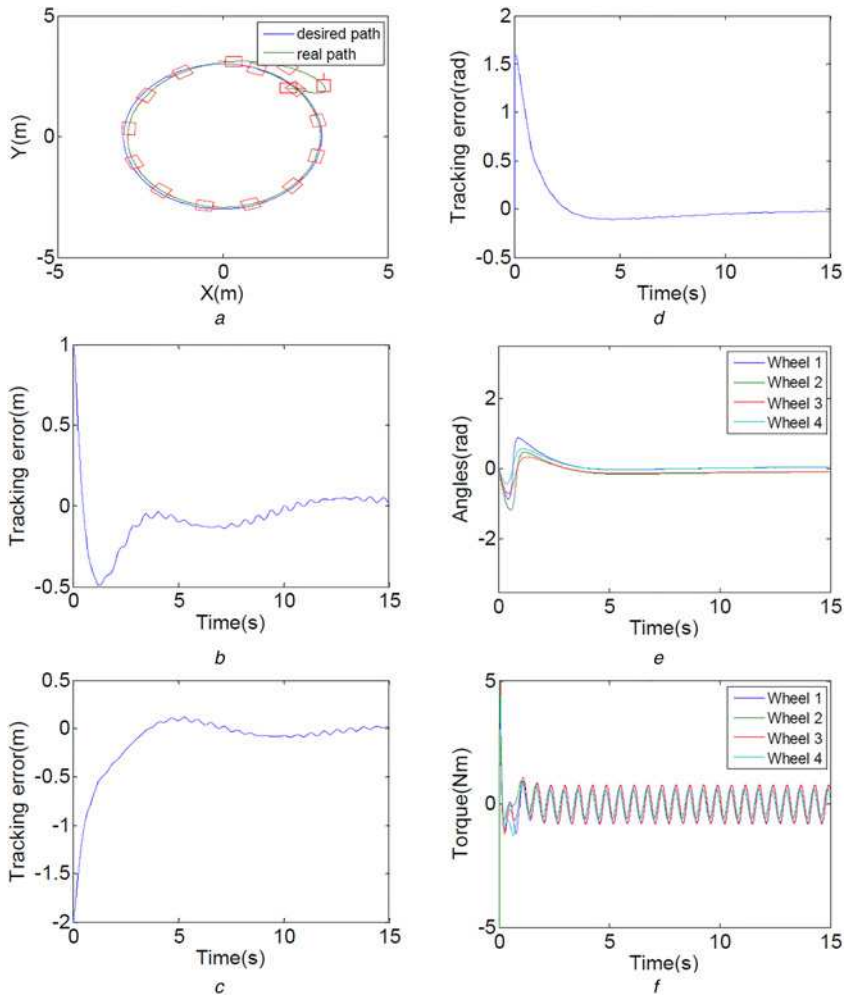


Fig. 8 *Simulation results of Case (I) by the PI dynamic controller*
a x–y plot of the 4WIS4WID mobile robot
b–d Tracking errors of x_e, y_e and θ_e
e Steering angle of four wheels
f Rolling torques of four wheels

4.3 *Comparative study*

The purpose of this section is to demonstrate the superiority of the proposed controller, where the kinematic controller is unchanged and the SMC dynamic controller is replaced by the PI controller. The control law (39) is rewritten as $\boldsymbol{\tau}(t) = \boldsymbol{K}_P\boldsymbol{e} + \boldsymbol{K}_I\int_0^t \boldsymbol{e}(\tau)\,\mathrm{d}\tau$, where $\boldsymbol{K}_P = \mathrm{diag}\{5, 5, 5, 5, 2, 2, 2, 2\}$ and $\boldsymbol{K}_I = \mathrm{diag}\{0.5, 0.5, 0.5, 0.5, 0.5, 0.5, 0.5, 0.5\}$. For the Case (I), the simulation results of the PI dynamic controller are depicted in Fig. 8. By comparing Fig. 6 with Fig. 8, one can find that the convergent speed of the tracking errors in Fig. 8 is slower than that in Fig. 6. Furthermore, the tracking errors of y_e and θ_e have some tremors in Fig. 8 and these phenomena are influenced by $\boldsymbol{D}(t)$. It shows that using the SMC is better than PI control to suppress the uncertainties and disturbances in this research.

5 Conclusions

This paper has proposed new kinematic and the dynamic models for 4WIS4WID mobile robot. These two models can be used to examine some new control schemes and/or other applications for the 4WIS4WID mobile robot. On the basis of these models, the dynamic trajectory tracking control for the 4WIS4WID mobile robot has been presented. The control scheme does not include the parameters of the ICR, so the discontinuous condition when the 4WIS4WID mobile robot moves straight does not encounter. To obtain a better performance for the trajectory tracking control, the proposed kinematic control scheme is derived by the non-linear control and the dynamic control scheme is established by the SMC control technique. Once all of the controller parameters are assigned correctly, the control law can reduce the trajectory tracking errors and suppress the affection of the system uncertainties and external disturbances efficiently. Using the Lyapunov stability theory, the stabilities of the kinematic and dynamic controllers have been proved. The simulation results demonstrate that whether the desired path is a straight line or curvilinear path, the 4WIS4WID mobile robot can track the path successfully. In comparison with the PI dynamic control, the SMC control is indeed effective in suppressing the influences of uncertainties and disturbances for the trajectory tracking control of 4WIS4WID mobile robot.

6 Acknowledgments

This work supported in part by the Ministry of Science and Technology of the Republic of China under grant NSC101-2221-E-006-193-MY3, in part by the Ministry of Education, and the aim for the Top University Project to the National Cheng Kung University (NCKU) are greatly appreciated.

This is an open access article published by the IET under the Creative Commons Attribution License (http://creativecommons.org/licenses/by/3.0/)

20513305, 2015, 1, Downloaded from https://ietresearch.onlinelibrary.wiley.com/doi/10.1049/joe.2014.0241, Wiley Online Library on [26/08/2026]. See the Terms and Conditions (https://onlinelibrary.wiley.com/terms-and-conditions) on Wiley Online Library for rules of use; OA articles are governed by the applicable Creative Commons License

7 References

[1] Yeh Y.C., Li T.H.S., Chen C.Y.: 'Adaptive fuzzy sliding-mode control of dynamic model based car-like mobile robot', *Int. J. Fuzzy Syst.*, 2009, **11**, (4), pp. 272–286

[2] Egerstedt M., Hu X., Stotsky A.: 'Control of mobile platforms using a virtual vehicle approach', *IEEE Trans. Autom. Control*, 2001, **46**, (11), pp. 1777–1782

[3] Hwang C.L., Chang N.W.: 'Fuzzy decentralized sliding-mode control of a car-like mobile robot in distributed sensor-network spaces', *IEEE Trans. Fuzzy Syst.*, 2008, **16**, (1), pp. 97–109

[4] Kumar U., Sukavanam N.: 'Backstepping based trajectory tracking control of a four wheeled mobile robot', *Int. J. Adv. Robot. Syst.*, 2008, **5**, (4), pp. 403–410

[5] Nishihara T.O., Kumamoto H.: 'Automatic path-tracking controller of a four-wheel steering vehicle', *Veh. Syst. Dyn.*, 2009, **47**, (10), pp. 1205–1227

[6] Song Y.D., Chen H.N., Li D.Y.: 'Virtual-point-based fault-tolerant lateral and longitudinal control of 4 W-steering vehicles', *IEEE Trans. Intell. Transp. Syst.*, 2011, **12**, (4), pp. 1343–1351

[7] Ruiz U., Murrieta-Cid R., Marroquin J.L.: 'Time-optimal motion strategies for capturing an omnidirectional evader using a differential drive robot', *IEEE Trans. Robot.*, 2013, **29**, (5), pp. 1180–1196

[8] Ailon A., Zohar I.: 'Control strategies for driving a group of nonholonomic kinematic mobile robots in formation along a time-parameterized path', *IEEE/ASME Trans. Mechatronics*, 2012, **17**, (2), pp. 326–336

[9] Zhang Q., Lapierre L., Xiang X.: 'Distributed control of coordinated path tracking for networked nonholonomic mobile vehicles', *IEEE Trans. Ind. Inform.*, 2013, **9**, (1), pp. 472–484

[10] Park B.S., Yoo S.J., Park J.B., Choi Y.H.: 'A bioinspired neurodynamics-based approach to tracking control of mobile robots', *IEEE Trans. Ind. Electron.*, 2012, **59**, (8), pp. 3211–3220

[11] Censi A., Franchi A., Marchionni L., Oriolo G.: 'Simultaneous calibration of odometry and sensor parameters for mobile robots', *IEEE Trans. Robot.*, 2013, **29**, (2), pp. 475–492

[12] Yi J., Wang H., Zhang J., Song D., Jayasuriya S., Liu J.: 'Kinematic modeling and analysis of skid-steered mobile robots with applications to low-cost inertial-measurement-unit-based motion estimation', *IEEE Trans. Robot.*, 2009, **25**, (5), pp. 1087–1097

[13] Yi J., Song D., Zhang J., Goodwin Z.: 'Adaptive trajectory tracking control of skid-steered mobile robots'. Proc. IEEE Int. Conf. on Robotics and Automation, 2007, pp. 2605–2610

[14] Morales J., Martinez J.L., Mandow A., Garcia-Cerezo A., Pedraza S.: 'Power consumption modeling of skid-steer tracked mobile robots on rigid terrain', *IEEE Trans. Robot.*, 2009, **25**, (5), pp. 1098–1108

[15] Kim K.B., Kim B.K.: 'Minimum-time trajectory for three-wheeled omnidirectional mobile robots following a bounded-curvature path with a referenced heading profile', *IEEE Trans. Robot.*, 2011, **27**, (4), pp. 800–808

[16] Indiveri G.: 'Swedish wheeled omnidirectional mobile robots: kinematics analysis and control', *IEEE Trans. Robot.*, 2009, **25**, (1), pp. 164–171

[17] Lins Barreto S.J.C., Scolari Conceicao A.G., Dorea C.E.T., Martinez L., de Pieri E.R.: 'Design and implementation of model-predictive control with friction compensation on an omnidirectional mobile robot', *IEEE/ASME Trans. Mechatronics*, 2014, **19**, (2), pp. 467–476

[18] Huang H.C.: 'SoPC-based parallel ACO algorithm and its application to optimal motion controller design for intelligent omnidirectional mobile robots', *IEEE Trans. Ind. Inform.*, 2013, **9**, (4), pp. 1828–1835

[19] Dietrich A., Wimbock T., Albu-Schaffer A., Hirzinger G.: 'Reactive whole-body control: dynamic mobile manipulation using a large number of actuated degrees of freedom', *IEEE Robot. Autom. Mag.*, 2012, **19**, (2), pp. 20–33

[20] Qian H., Lam T.L., Li W., Xia C., Xu Y.: 'System and design of an omni-directional vehicle'. Proc. IEEE Int. Conf. on Robotics and Biomimetics, Bangkok, Thailand, 2009, pp. 389–394

[21] Connette C.P., Pott A., Hägele M., Verl A.: 'Control of an pseudo-omnidirectional, non-holonomic, mobile robot based on an ICM representation in spherical coordinates'. Proc. IEEE Int. Conf. on Decision and Control, Cancun, Mexico, 2008, pp. 4976–4983

[22] Clavien L., Lauria M., Michaud F.: 'Instantaneous centre of rotation estimation of an omnidirectional mobile robot'. Proc. IEEE Int. Conf. on Robotics and Automation, Anchorage, AK, USA, 2010, pp. 5435–5440

[23] Ploeg J., van der Knaap A.C.M., Verburg D.J.: 'ATS/AGV-design, implementation and evaluation of a high performance AGV'. Proc. IEEE Intelligent Vehicles Symp., 2002, **1**, pp. 127–134

[24] Lin C.J., Hsiao S.M., Wang Y.H., Yeh C.H., Huang C.F., Li T.H.S.: 'Design and implementation of a 4WS4WD mobile robot and its control applications'. Proc. IEEE Int. Conf. on Systems Science and Engineering, Budapest, Hungary, 2013, pp. 235–240

[25] Lam T.L., Qian H., Xu Y.: 'Omnidirectional steering interface and control for a four-wheel independent steering vehicle', *IEEE/ASME Trans. Mechatronics*, 2010, **15**, (3), pp. 329–338

[26] Jiang S.Y., Song K.T.: 'Differential flatness-based motion control of a steer-and-drive omnidirectional mobile robot'. Proc. IEEE Int. Conf. on Mechatronics and Automation 2013, Takamatsu, Japan, August 2013, pp. 1167–1172

[27] Selekwa M.F., Nistler J.R.: 'Path tracking control of four wheel independently steered ground robotic vehicles'. Proc. IEEE Conf. on Decision and Control and European Control Conf. (CDC-ECC), Orlando, FL, USA, December 2011, pp. 6355–6360

[28] Hwang C.L., Wu H.M.: 'Trajectory tracking of a mobile robot with frictions and uncertainties using hierarchical sliding-mode under-actuated control', *IET Control Theory Appl.*, 2013, **7**, (7), pp. 952–965

[29] Jean J.H., Lian F.L.: 'Robust visual servo control of a mobile robot for object tracking using shape parameters', *IEEE Trans. Control Syst. Technol.*, 2012, **20**, (6), pp. 1461–1472

[30] Rubagotti M., Della Vedova M.L., Ferrara A.: 'Time-optimal sliding-mode control of a mobile robot in a dynamic environment', *IET Control Theory Appl.*, 2011, **5**, (16), pp. 1916–1924

This is an open access article published by the IET under the Creative Commons Attribution License (http://creativecommons.org/licenses/by/3.0/)

20513305, 2015, 1, Downloaded from https://ietresearch.onlinelibrary.wiley.com/doi/10.1049/joe.2014.0241, Wiley Online Library on [26/08/2026]. See the Terms and Conditions (https://onlinelibrary.wiley.com/terms-and-conditions) on Wiley Online Library for rules of use; OA articles are governed by the applicable Creative Commons License